How to cite: *Angew. Chem. Int. Ed.* **2025**, *64*, e202419675
doi.org/10.1002/anie.202419675

VIP Bioinorganic Catalysis Very Important Paper

Mimicking the CO_2-Bound State of the [Ni,Fe]-CO Dehydrogenase

*Siad Wolff, Arne Hofmann, Konstantin B. Krause, Kilian Weisser, Beatrice. Cula, Thomas Lohmiller, Christian Herwig, and Christian Limberg**

Abstract: Complexes, where a doubly reduced CO_2^{2-} (carbonite) ligand is spanned between a nickel(II) centre and a transition metal(II) ion (TM=Fe, Co, Zn) have been accessed. In non-coordinating solvents the carbonite ligand exhibits a flexible coordination behaviour as observed by NMR spectroscopy and supported by DFT calculations. In particular the [Ni-CO_2-Fe] representative replicates the respective entity in an intermediate formed during CO_2-conversion by the enzyme [Ni,Fe]-CODH in many ways (structure, spectroscopic properties, reactivity). Our investigations reveal that transition metal ions reduce the reduction potential of the carbonite unit but increase its tendency to undergo C–O bond cleavage. This may explain the choice of an iron(II) ion instead of a s- or p-block-based Lewis acid as part of the active site.

The [Ni,Fe]-containing carbon monoxide dehydrogenase ([Ni,Fe]-CODH) represents a natural blue-print for CO_2 activating systems.[1] These enzymes are employed by bacteria as catalysts for the reversible transformation of CO_2 to CO with high turnover frequencies and almost no overpotential.[2] The conversion occurs at a nickel centre embedded in an iron-sulphide environment, supported by a Lewis acid, namely, a high-spin Fe^{II} centre, the so-called ferrous-component II (FCII).[1a,3] Dobbek and co-workers have achieved the crystallisation and structural characterisation of the intermediate C_{red2}-CO_2 in which a doubly reduced CO_2^{2-} ligand, coined carbonite,[4] is bound in a Ni^{II}-(μ_2-CO_2-$\kappa C:\kappa O$)-Fe^{II} fashion.[5]

[*] S. Wolff, A. Hofmann, Dr. K. B. Krause, K. Weisser, Dr. B. Cula, Dr. T. Lohmiller, Dr. C. Herwig, Prof. Dr. C. Limberg
Institut für Chemie
Humboldt-Universität zu Berlin
Brook-Taylor-Straße 2, 12489 Berlin (Germany)
E-mail: christian.limberg@chemie.hu-berlin.de

Dr. T. Lohmiller
EPR4Energy Joint Lab, Department Spins in Energy Conversion and Quantum Information Science, Helmholtz-Zentrum Berlin für Materialien und Energie GmbH
Albert-Einstein-Straße 16, 12489 Berlin (Germany)

While these findings concerning the CODH are inspiring the field of CO_2 activation, the electronic structures of the intermediates and the role of FCII remain debated.[1b,2b, 6] Investigations on biomimetic model complexes can contribute valuable information to such discussions, as they may help explaining certain structural features, the role of components in the active site and the behaviour of postulated intermediates.[7] However, despite the high interest in the CODH, molecular compounds that replicate the CO_2-bound state of the [Ni,Fe]-CODH, i.e. featuring a Ni-CO_2-Fe moiety, are hardly known. In fact, the only example of a Ni-CO_2-Fe complex was reported by Lee and coworkers in 2017 (Figure 1, **X**).[8] This scarcity of structural model complexes certainly arises from synthetic difficulties attributed to the high reactivity of metal-bound CO_2 complexes.[9]

The iron-sulphur cluster surrounding the nickel atom in the CODH mainly determines the electronic situation at the metal and also serves as a reductant. We have shown that with β-diketiminato coligands (L^{tBu}) complexes bearing Ni^{II}-CO_2^{2-} moieties can be generated that mimic structural features of the intermediate C_{red2}-CO_2 like the exceptionally short Ni–C bond and also the reactivity with protons (leading to CO formation). Notably, these complexes can be accessed either starting with nickel(0) by CO_2 activation, or, alternatively and more conveniently, via deprotonation of a β-diketiminato Ni^{II} formate precursor [L^{tBu}NiOOCH].[10] In the carbonite complexes [L^{tBu}Ni(CO_2)AM] thus obtained the charge is compensated by an alkali metal ion (AM=Li, Na, K), resulting in a bifunctional system where the carbonite ligand is activated between the Ni centre and the Lewis acidic AM support.[11] Most recently we reported that the AM counter ion can be exchanged by group II metal ions using a salt metathesis approach.[12] In the present contribution we make use of what we have learned in this previous work to accomplish the introduction of transition metal ions as the Lewis acidic counterions, in particular high-spin Fe^{II}, to emulate the enzymatic intermediate even more closely.

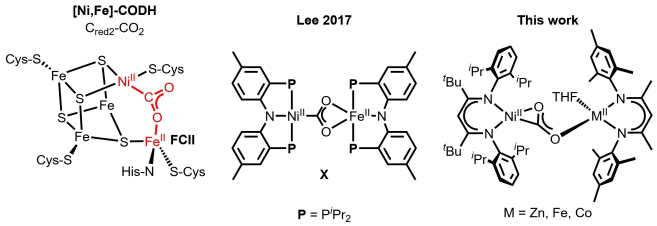

Figure 1. Structure of the C_{red2}-CO_2 state of the [Ni, Fe]-CODH (left) and its molecular models.

Based on the previous experiences with earth alkaline metal ions a salt metathesis approach was pursued, and for the saturation of the residual coordination sphere at the transition metal centres (M) a β-diketiminato ligand was chosen. As mentioned, a strong focus was on iron(II), but to establish a viable synthetic procedure to access the target molecule with a paramagnetic [$L^{tBu}Ni(CO_2)FeL^{Mes}$] entity, first of all the corresponding zinc compound was targeted, as this enabled evaluation of the reaction course via NMR spectroscopy. Following our previously reported route to a [Ni,Mg]-derivative,[12] initial attempts were performed using zinc halide precursors [$L^{Mes}ZnX$] (X=Cl, Br, I) for a salt metathesis with [Ni,AM]-carbonite complexes, however, in no case a conversion was observed. Hence, the more electrophilic Zn precursor [$L^{Mes}Zn(OTf)THF$], $\mathbf{1^{Zn}}$, with a weakly coordinating triflate ligand was synthesised (Scheme 1) to facilitate the exchange reaction.

Indeed, reaction of [$L^{tBu}Ni(CO_2)Na$] with $\mathbf{1^{Zn}}$ gave [$L^{tBu}Ni(CO_2)Zn(THF)L^{Mes}$], $\mathbf{2^{Zn}}$, as clearly indicated by NMR spectroscopy (SI section 2.5). Based on this finding also the syntheses of $\mathbf{2^{Fe}}$ and $\mathbf{2^{Co}}$ were achieved using analogous precursors (Scheme 1). Single crystal X-ray analysis showed that all three derivatives are isostructural, exhibiting the same μ_2-$\kappa^2C,O:\kappa O'$ coordination of the carbonite ligand (Figure 2). A THF solvent molecule was found to be coordinated (besides L^{Mes} and carbonite) at the

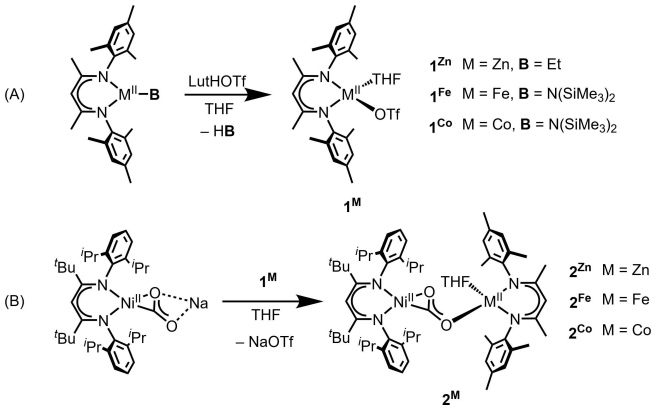

Scheme 1. Synthesis of complexes $\mathbf{1^M}$ (A) and their reaction with [$L^{tBu}Ni(CO_2)Na$] to form $\mathbf{2^M}$ (B).

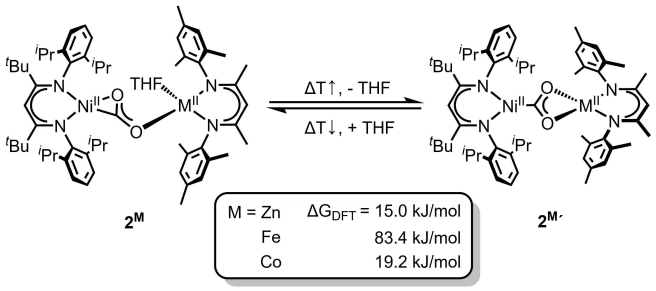

Scheme 2. Temperature-dependent interconversion of $\mathbf{2^M}$ and $\mathbf{2^{M'}}$ and the calculated Gibbs free energies (ΔG_{DFT}) for THF liberation from $\mathbf{2^M}$.

M sites leading to a tetrahedral coordination for all derivatives.

Although $\mathbf{2^{Mg}}$ and $\mathbf{2^{Zn}}$ share a very similar solid-state structure, NMR spectroscopic investigations revealed that in non-coordinating solvents the THF ligand of $\mathbf{2^{Zn}}$ (unlike the one in $\mathbf{2^{Mg}}$) is rather labile and can be cleaved off at elevated temperatures to yield [$L^{tBu}Ni(CO_2)ZnL^{Mes}$], $\mathbf{2^{Zn'}}$(see Supporting Information section 3), which shows at 65 °C just one sharp signal set for all iso-propyl and tert-butyl residues of the L^{tBu} ligand, indicating an on average C_{2v}-symmetric structure and thus a μ_2-$\kappa C:\kappa^2 O,O'$ coordination mode of the carbonite ligand within $\mathbf{2^{Zn'}}$. Lowering the temperature leads to a broadening of the signals before two sharp signal sets are visible, as expected based on the structure of $\mathbf{2^{Zn}}$ (Scheme 2); the point of coalescence is 25 °C and the energy barrier for the transformation $\mathbf{2^{Zn}}\rightarrow\mathbf{2^{Zn'}}$/THF as estimated using the Eyring equation amounts to 61.4 kJ/mol (see Supporting Information section 3).

Attempts to isolate $\mathbf{2^{Zn'}}$ failed, since extensive drying at elevated temperatures led to continuous decomposition of $\mathbf{2^{Zn}}$. Therefore, DFT calculations were performed to substantiate the experimental findings. Structure optimisation of $\mathbf{2^{Zn'}}$ confirmed that upon THF dissociation a κ^2O,O' coordination at the Zn ion is the most favourable one (Figure 3 and Supporting Information section 9). Surprisingly, the Ni1–O1 bond in the original structure of $\mathbf{2^{Zn}}$ is significantly elongated but not completely cleaved in the DFT-optimised structure, so that there is no C_s-symmetry (Table 1). We assume that in solution the carbonite ligand exhibits a fluctuating interaction of both O-atoms with the

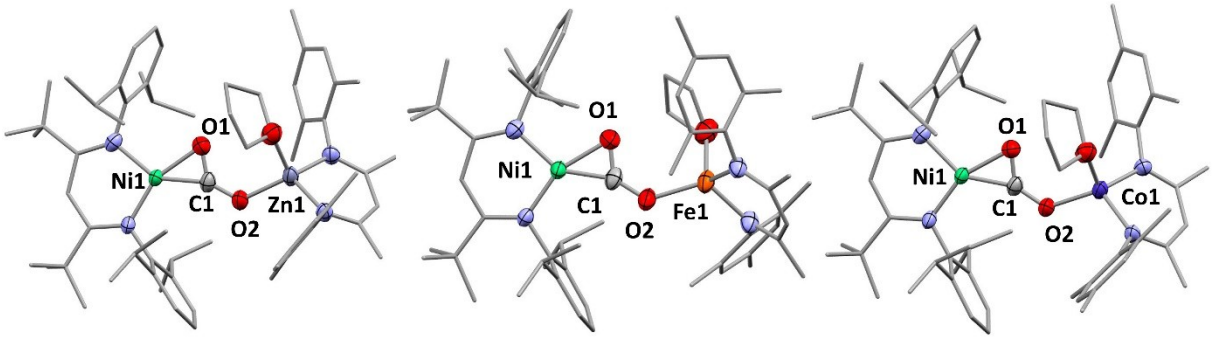

Figure 2. Molecular structures of complexes $\mathbf{2^M}$. Hydrogen atoms are omitted for clarity. For selected bond length and angles see Table 1.

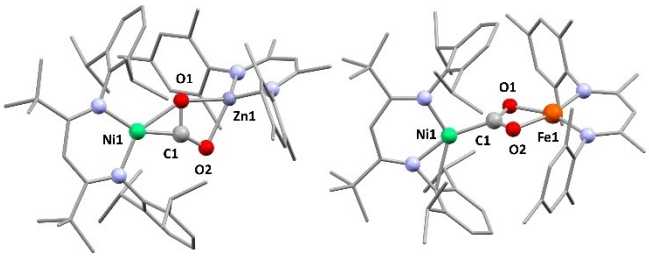

Figure 3. DFT-Optimised structures of $\mathbf{2}^{\mathbf{Zn_I}}$ (left) and $\mathbf{2}^{\mathbf{Fe_I}}$ (right). Hydrogen atoms are omitted for clarity. $\mathbf{2}^{\mathbf{Co_I}}$ is isostructural to $\mathbf{2}^{\mathbf{Zn_I}}$ (see Supporting Information Figure S88). For selected bond length and angles see Table 1 or Supporting Information Table S9.

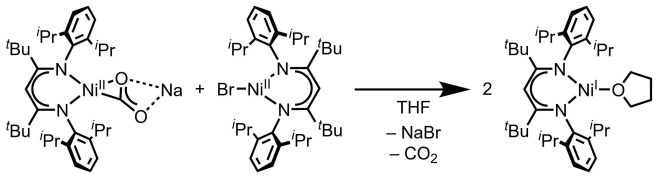

Scheme 3. Reaction between [$L^{tBu}Ni(CO_2)Na$] and [$L^{tBu}NiBr$].

Ni centre, resulting in a C_{2v} symmetric structure on the NMR time scale. In accordance with the observed temperature-dependency the free enthalpy for the interconversion $\mathbf{2}^{\mathbf{Zn}}\rightarrow\mathbf{2}^{\mathbf{Zn_I}}$/THF was calculated to be 15 kJ/mol, indicating a slightly endergonic process (Scheme 2).

Due to their paramagnetic nature $\mathbf{2}^{\mathbf{Fe}}$ and $\mathbf{2}^{\mathbf{Co}}$ could not be investigated by NMR spectroscopy, so that the potential THF liberation was studied solely via computational methods. While calculations for $\mathbf{2}^{\mathbf{Co}}$ gave similar results compared to the Zn-derivative, optimisation of $\mathbf{2}^{\mathbf{Fe_I}}$ yielded a very different structure with a clear κ*C* coordination at the nickel site (Figure 3). However, the dissociation $\mathbf{2}^{\mathbf{Fe}}\rightarrow\mathbf{2}^{\mathbf{Fe_I}}$/THF was found to be significantly more endergonic, suggesting that it does not occur in solution and that correspondingly $\mathbf{2}^{\mathbf{Fe}}$ does not feature a carbonite rearrangement. This difference in behaviour compared to the Zn and Co derivatives can be rationalised by the more pronounced oxophilic character of Fe,[13] inhibiting the liberation of coordinated THF.

As $\mathbf{2}^{\mathbf{Fe}}$ and $\mathbf{2}^{\mathbf{Co}}$ feature open-shell metal sites, the electronic structures of both complexes were investigated. The Mössbauer spectrum of $\mathbf{2}^{\mathbf{Fe}}$ displays a doublet with an isomer shift (δ) of 0.98 mm/s and a quadrupole splitting (ΔE_Q) of 2.09 mm/s, consistent with a high-spin Fe^{II} site (see Supporting Information section 6). The EPR spectrum of $\mathbf{2}^{\mathbf{Co}}$ shows a signal characteristic for a tetrahedral high-spin Co^{II} site (see Supporting Information section 7). SQUID measurements revealed that $\mathbf{2}^{\mathbf{Fe}}$ and $\mathbf{2}^{\mathbf{Co}}$ exhibit a room-temperature magnetic moment somewhat above the spin-only values for $S=2$ and $S=3/2$ states, respectively, suggesting that all unpaired electrons are located at the Fe/Co centres (see Supporting Information section 8). Therefore, no intramolecular redox-events (electron transfers) occur within the Ni^{II}-CO_2^{2-}-M^{II} cores, indicating that the Fe^{II} and Co^{II} centres exclusively act as Lewis acids. Interestingly, when trying to generate a homobimetallic [Ni,Ni] carbonite by reacting [$L^{tBu}Ni(CO_2)Na$] with [$L^{tBu}NiBr$] a redox reaction was observed leading to [$L^{tBu}Ni(THF)$] and release of CO_2 (Scheme 3 and Supporting Information section 2.14). Apparently, the higher electronegativity of the Ni^{II} centre compared to Fe^{II}/Co^{II} triggers the release of the two electrons stored within the carbonite ligand to reduce both $L^{tBu}Ni^{II}$ moieties.

Having observed that the carbonite complexes can act as reductants their chemical behaviour toward other $1e^-$-oxidants was tested. While [$L^{tBu}Ni(CO_2)Na$] was able to reduce [$CoCp_2$][PF_6] with concomitant formation of [$L^{tBu}Ni(THF)$] and CO_2, no redox reaction could be observed when mixing [$CoCp_2$][PF_6] with complexes $\mathbf{2}^{\mathbf{M}}$, indicating a difference in reduction potentials (SI section 4.1 and 4.3). Hence, CV studies were performed to understand the redox properties of the carbonites. A detailed description of the collected data can be found in the Supporting Information (section 4),

Table 1: Spectroscopic and metric data of the [Ni,Fe]-CODH and respective carbonite model complexes. Bond lengths and angles are given in [Å] and [°].

	[Ni,Fe]-CODH[a] (C_{red2}-CO_2)	$\mathbf{2}^{\mathbf{Mg}}$ [b]	$\mathbf{2}^{\mathbf{Zn}}$	$\mathbf{2}^{\mathbf{Zn_I}}$ [c]	$\mathbf{2}^{\mathbf{Fe}}$	$\mathbf{2}^{\mathbf{Co}}$	**X**[8]
δ_{13C} [ppm]	–	175.8	174.63	178.46	–	–	–
ν_{CO2} [cm^{-1}]	1724, 1741	1577	1573	–	1577	1577	1510
d(Ni1–C1)	1.805(31)	1.839(2)	1.815(3)	1.823	1.803(3)	1.819(2)	1.858(1)
d(Ni1–O1)	–	1.925(2)	1.933(2)	2.120	1.929(2)	1.931(2)	–
d(C1–O1)	1.298(30)	1.269(4)	1.254(4)	1.306	1.259(4)	1.258(4)	1.269(2)
d(C1–O2)	1.316(30)	1.236(3)	1.265(4)	1.255	1.269(4)	1.264(3)	1.289(2)
d(M–O1)	–	–	–	2.099	–	–	2.204(1)
d(M–O2)	2.030(18)	1.974(2)	1.976(2)	2.081	1.988(2)	1.980(2)	2.066(1)
∠(O1-C1–O2)	117.9(2.6)	129.3(3)	128.5(3)	119.4	127.3(3)	128.6(2)	116.5(1)
δ [mm/s]	0.82	–	–	–	0.98	–	–
ΔE_Q [mm/s]	2.82	–	–	–	2.09	–	–

(a) Structural data by Dobbek et al.[5a] IR spectroscopic data by Bagley et al.[15] Mössbauer data for C_{red1} by Münck et al.[16] (b) data reported in a previous paper[12] (c) DFT-optimised model (see SI).

while this discussion will focus on the oxidative waves of [L^{tBu}Ni(CO$_2$)Na] and **2^M**, as these are closely associated with the carbonite ligands. [L^{tBu}Ni(CO$_2$)Na] features an irreversible oxidation at −1.10 V (**I**) which is assigned to an oxidation of the CO_2^{2-} ligand (Figure 4, red line). This event is followed by a reversible oxidation at −1.07 V (**II/II'**) assigned to the Ni^I/Ni^{II} redox couple of [L^{tBu}Ni(THF)], forming upon decomposition after event **I**. Complexes **2^M** display a very different electrochemical behaviour featuring an irreversible oxidation at about −0.35 V (**I***, Figure 4, blue line showing exemplarily the curve of **2^{Co}**). Hence, exchange of the Na^+ counterion by $[L^{Mes}M]^+$ moieties shifts the reduction potential of complexes **2^M** to more positive potentials by about 0.8 V. This difference in reduction potential can be explained by a stronger delocalisation of charge/electron density within the Ni^{II}-CO_2^{2-}-M^{II} cores, inhibiting e^- transfer.

Furthermore, the L^{Mes}M-moieties also significantly affect the stability of the Ni carbonites. Complexes **2^M** readily decompose within a few days at room-temperature via C–O bond cleavage to yield [L^{tBu}NiCO] and [L^{tBu}Ni(CO$_3$)M-(THF)L^{Mes}], **3^M**, as main products (Scheme 4). In contrast, the [Ni,AM] derivatives are rather stable under inert conditions and can be stored for several days; C–O bond cleavage was only observed upon addition of electrophiles (H^+, Me_3Si^+, CO_2).[10–11] As such external triggers are not required for complexes **2^M**, they obviously exhibit significantly stronger activation of the carbonite ligands, which intrinsically are already at the edge of C–O bond cleavage. This is corroborated by a large red shift of the C–O stretching frequencies (ν_{CO2}) for all derivatives supported by divalent metal ions, indicating high degrees of activation (Table 1).

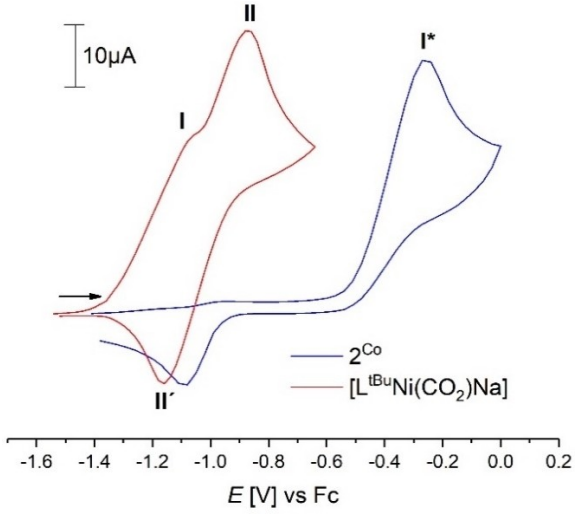

Figure 4. Superimposed CV curves for [L^{tBu}Ni(CO$_2$)Na] and **2^{Co}** in THF/0.1 M [Bu$_4$N][PF$_6$], scan rate 100 mV/s.

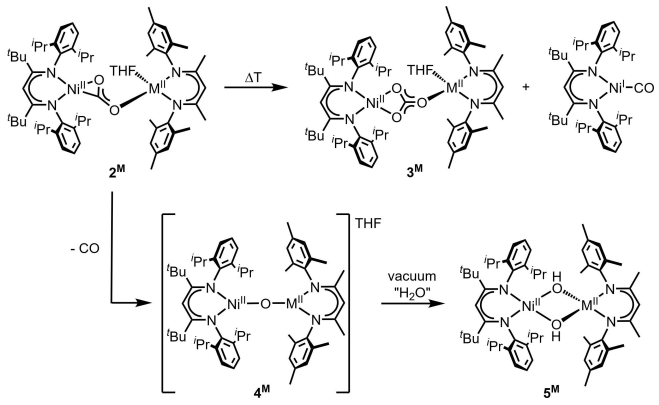

Scheme 4. Decomposition of **2^M**.

Naturally, the initial step of the decomposition of **2^M** is the liberation of CO, which should yield a Ni(II)-oxo-M(II) complex [L^{tBu}Ni(μ-O)ML^{Mes}], **4^M**. The released CO itself triggers a cascade of reactions, eventually leading to the final product mixture (for detailed analysis of the reaction course see Supporting Information section 5). In an attempt to trap the oxo-intermediate **4^M**, decomposition of complexes **2^M** was performed under dynamic vacuum to avoid subsequent reactions with CO. However, this led to the isolation of [L^{tBu}Ni(μ-OH)$_2$ML^{Mes}], **5^M**, instead of **4^M**. Ni-oxo species are usually considered as highly reactive.[14] Hence, it is assumed that formation of **5^M** proceeds via reaction of transient **4^M** with trace amounts of H_2O (Scheme 4).

Taken together, the Ni-CO_2-Fe entity within **2^{Fe}** closely mimics the respective moiety in the enzymatic intermediate C_{red2}-CO_2 (Table 1). Crystallographic data of this enzymatic state had revealed an exceptionally short Ni–C bond (1.805 (31) Å), which is very well reproduced by **2^{Fe}** (1.803(3) Å) and can be rationalized by a partial carbene character of the carbonite ligand.[5a,10a] The only other known Ni–CO_2–Fe complex, **X**, reported by Lee and co-workers, features a significantly longer Ni–C bond (1.858(1) Å). It reproduces the strong O–C–O bending and the η^1-κC coordination of the carbonite ligand, though, which is bound in a η^2-κC,O mode in **2^{Fe}**. The Mössbauer data of FCII present in C_{red2}-CO_2 have not been reported yet but they are likely similar to those of the 2e$^-$-oxidised state C_{red1}.[16] Here the ΔE_Q value is somewhat larger due to the presence of four inequivalent ligands while the iron centre in **2^{Fe}** is coordinated by a symmetric bidentate β-diketiminate. The δ values are both in the typical region for high-spin iron(II) centres. While investigations on the reactivity of **X** were impeded by its instability,[8] we found that **2^{Fe}** nicely replicates the chemical behaviour of C_{red2}-CO_2: In contact with a proton (LutH(OTf) in case of **2^{Fe}**, see Supporting Information section 5.4) CO is released. CO formation proceeds even without an electrophilic trigger, which emphasises the strong activation of CO_2 spanned between the nickel and iron ions, that is also reflected in the CV measurements: The push-pull effect delocalises the charge and leads to a comparatively high oxidation potential. Considering the various common features between C_{red2}-CO_2 and **2^{Fe}** it is worthwhile to also compare the vibrational absorptions. In a unique study from 2003 a band at about 1730 cm^{-1} was assigned to the CO_2 bound state in [Ni,Fe]-CODH; no other information is available.[15] However, this spectral region is more characteristic for CO_2 ligands at nickel that are only weakly

activated,[17] while the CODH is considered to feature a strongly activated carbonite ligand.[5] The presented carbonite complex $\mathbf{2^{Fe}}$ exhibits a C–O stretching frequency at 1577 cm^{-1} indicating strong activation of the CO_2 molecule. Insofar we propose that the assignment of the band in the CODH work to a CO_2 adduct was not correct. Instead, a Ni^0-carbonyl species would be conceivable (for instance, $K_2[L^{tBu}Ni^0CO]_2$ absorbs at 1715 cm^{-1}).[18] Ni^0-carbonyls do not represent intermediates in the catalytic cycle of the CODH but it may be possible that such species accumulated under the experimental conditions in the previous work.

In conclusion we report here novel nickel(II)-carbonite-transition-metal(II) complexes, which feature a strongly activated CO_2 ligand, as indicated by the short Ni–C bonds, the position of ν_{CO} bands, CV measurements, as well as the chemical behaviour. In particular the [Ni,Fe] representative thus resembles C_{red2}-CO_2 in many ways. For our studies an inverse relation between redox behaviour and activation emerged: transition metal ions reduce the reduction potential of the carbonite unit but increase its tendency to undergo C–O bond cleavage. It may thus be inferred that also FCII on the one hand supports the activation, so that a mild decrease of pH can trigger CO formation, and on the other hand prevents electron transfer from the carbonite unit.

Supporting Information

The authors have cited additional references within the Supporting Information.[19–41]

Acknowledgements

Funded by the Deutsche Forschungsgemeinschaft (DFG, German Research Foundation) under Germany's Excellence Strategy – EXC 2008/1-390540038. T.L. also acknowledges support by DFG (Project No. LO 2898/1-1). Open Access funding enabled and organized by Project DEAL. Open Access funding enabled and organized by Projekt DEAL.

Conflict of Interest

The authors declare no conflict of interest.

Data Availability Statement

The data that support the findings of this study are available in the supplementary material of this article.

Keywords: CODH · CO_2 activation · Bimetallic · nickel β-diketiminate

[1] a) M. Can, F. A. Armstrong, S. W. Ragsdale, *Chem. Rev.* **2014**, *114*, 4149–4174; b) A. M. Appel, J. E. Bercaw, A. B. Bocarsly, H. Dobbek, D. L. DuBois, M. Dupuis, J. G. Ferry, E. Fujita, R. Hille, P. J. A. Kenis, C. A. Kerfeld, R. H. Morris, C. H. F. Peden, A. R. Portis, S. W. Ragsdale, T. B. Rauchfuss, J. N. H. Reek, L. C. Seefeldt, R. K. Thauer, G. L. Waldrop, *Chem. Rev.* **2013**, *113*, 6621–6658.

[2] a) S. A. Ensign, *Biochemistry* **1995**, *34*, 5372–5381; b) J. Ruickoldt, Y. Basak, L. Domnik, J.-H. Jeoung, H. Dobbek, *ACS Catal.* **2022**, *12*, 13131–13142.

[3] a) C. L. Drennan, J. Heo, M. D. Sintchak, E. Schreiter, P. W. Ludden, *Proc. Natl. Acad. Sci. USA* **2001**, *98*, 11973–11978; b) P. Amara, J.-M. Mouesca, A. Volbeda, J. C. Fontecilla-Camps, *Inorg. Chem.* **2011**, *50*, 1868–1878; c) P. A. Lindahl, *J. Inorg. Biochem.* **2012**, *106*, 172–178.

[4] A. Paparo, J. Okuda, *J. Organomet. Chem.* **2018**, *869*, 270–274.

[5] a) J. Fesseler, J. H. Jeoung, H. Dobbek, *Angew. Chem. Int. Ed.* **2015**, *54*, 8560–8564; b) J.-H. Jeoung, H. Dobbek, *Science* **2007**, *318*, 1461–1464.

[6] S. H. Newman-Stonebraker, T. J. Gerard, P. L. Holland, *Chem* **2024**, *10*, 1655–1667.

[7] a) S. C. Lee, W. Lo, R. H. Holm, *Chem. Rev.* **2014**, *114*, 3579–3600; b) A. Majumdar, *Dalton Trans.* **2014**, *43*, 12135–12145; c) S. Ogo, Y. Mori, T. Ando, T. Matsumoto, T. Yatabe, K.-S. Yoon, H. Hayashi, M. Asano, *Angew. Chem. Int. Ed.* **2017**, *56*, 9723–9726; d) J. R. Prat, C. A. Gaggioli, R. C. Cammarota, E. Bill, L. Gagliardi, C. C. Lu, *Inorg. Chem.* **2020**, *59*, 14251–14262; e) Ø. Hatlevik, M. C. Blanksma, V. Mathrubootham, A. M. Arif, E. L. Hegg, *J. Biol. Inorg. Chem.* **2004**, *9*, 238–246; f) M. E. Ahmed, S. Adam, D. Saha, J. Fize, V. Artero, A. Dey, C. Duboc, *ACS Energy Lett.* **2020**, *5*, 3837–3842; g) D. W. N. Wilson, M. S. Fataftah, Z. Mathe, B. Q. Mercado, S. DeBeer, P. L. Holland, *J. Am. Chem. Soc.* **2024**, *146*, 4013–4025.

[8] C. Yoo, Y. Lee, *Chem. Sci.* **2017**, *8*, 600–605.

[9] a) L. Roy, M. H. Al-Afyouni, D. E. DeRosha, B. Mondal, I. M. DiMucci, K. M. Lancaster, J. Shearer, E. Bill, W. W. Brennessel, F. Neese, S. Ye, P. L. Holland, *Chem. Sci.* **2019**, *10*, 918–929; b) B. Horn, C. Limberg, C. Herwig, B. Braun, *Chem. Commun.* **2013**, *49*, 10923–10925; c) J. P. Krogman, B. M. Foxman, C. M. Thomas, *J. Am. Chem. Soc.* **2011**, *133*, 14582–14585; d) R. Lalrempuia, A. Stasch, C. Jones, *Chem. Sci.* **2013**, *4*, 4383–4388.

[10] a) P. Zimmermann, S. Hoof, B. Braun-Cula, C. Herwig, C. Limberg, *Angew. Chem. Int. Ed.* **2018**, *57*, 7230–7233; b) P. Zimmermann, D. Ar, M. Rößler, P. Holze, B. Cula, C. Herwig, C. Limberg, *Angew. Chem. Int. Ed.* **2021**, *60*, 2312–2321.

[11] S. Wolff, V. Pelmenschikov, R. Muller, M. Ertegi, B. Cula, M. Kaupp, C. Limberg, *Chem. Eur. J.* **2024**, e202303112.

[12] S. Wolff, A. Ponsonby, A. Dallmann, C. Herwig, F. Beckmann, B. Cula, C. Limberg, *Chem. Commun.* **2024**, *60*, 5816–5819.

[13] a) G. O. Kayode, M. M. Montemore, *J. Mater. Chem. A* **2021**, *9*, 22325–22333; b) K. P. Kepp, *Inorg. Chem.* **2016**, *55*, 9461–9470; c) K. A. Moltved, K. P. Kepp, *J. Phys. Chem. C* **2019**, *123*, 18432–18444.

[14] a) S. Yao, Y. Xiong, M. Vogt, H. Grützmacher, C. Herwig, C. Limberg, M. Driess, *Angew. Chem. Int. Ed.* **2009**, *48*, 8107–8110; b) S. Yao, C. Herwig, Y. Xiong, A. Company, E. Bill, C. Limberg, M. Driess, *Angew. Chem. Int. Ed.* **2010**, *49*, 7054–7058; c) S. Yao, M. Driess, *Acc. Chem. Res.* **2012**, *45*, 276–287; d) S. Kundu, F. F. Pfaff, E. Miceli, I. Zaharieva, C. Herwig, S. Yao, E. R. Farquhar, U. Kuhlmann, E. Bill, P. Hildebrandt, H. Dau, M. Driess, C. Limberg, K. Ray, *Angew. Chem. Int. Ed.* **2013**, *52*, 5622–5626.

[15] J. Chen, S. Huang, J. Seravalli, H. Gutzman, D. J. Swartz, S. W. Ragsdale, K. A. Bagley, *Biochemistry* **2003**, *42*, 14822–14830.

[16] a) Z. Hu, N. J. Spangler, M. E. Anderson, J. Xia, P. W. Ludden, P. A. Lindahl, E. Münck, *J. Am. Chem. Soc.* **1996**, *118*, 830–845; b) P. A. Lindahl, S. W. Ragsdale, E. Münck, *J. Biol. Chem.* **1990**, *265*, 3880–3888; c) J. Xia, Z. Hu, C. V. Popescu, P. A. Lindahl, E. Münck, *J. Am. Chem. Soc.* **1997**, *119*, 8301–8312.
[17] a) J. S. Anderson, V. M. Iluc, G. L. Hillhouse, *Inorg. Chem.* **2010**, *49*, 10203–10207; b) M. Aresta, C. F. Nobile, V. G. Albano, E. Forni, M. Manassero, *J. Chem. Soc. Chem. Commun.* **1975**, 636–637.
[18] B. Horn, S. Pfirrmann, C. Limberg, C. Herwig, B. Braun, S. Mebs, R. Metzinger, *Z. Anorg. Allg. Chem.* **2011**, *637*, 1169–1174.
[19] A. Panda, M. Stender, R. J. Wright, M. M. Olmstead, P. Klavins, P. P. Power, *Inorg. Chem.* **2002**, *41*, 3909–3916.
[20] R. E. H. Kuveke, L. Barwise, Y. van Ingen, K. Vashisth, N. Roberts, S. S. Chitnis, J. L. Dutton, C. D. Martin, R. L. Melen, *ACS Cent. Sci.* **2022**, *8*, 855–863.
[21] N. J. Hartmann, G. Wu, T. W. Hayton, *Chem. Sci.* **2018**, *9*, 6580–6588.
[22] M. Biyikal, K. Löhnwitz, N. Meyer, M. Dochnahl, P. W. Roesky, S. Blechert, *Eur. J. Inorg. Chem.* **2010**, *2010*, 1070–1081.
[23] P. L. Holland, T. R. Cundari, L. L. Perez, N. A. Eckert, R. J. Lachicotte, *J. Am. Chem. Soc.* **2002**, *124*, 14416–14424.
[24] M. T. Huggins, T. Kesharwani, J. Buttrick, C. Nicholson, *J. Chem. Educ.* **2020**, *97*, 1425–1429.
[25] P. Zimmermann, A. F. R. Kilpatrick, D. Ar, S. Demeshko, B. Cula, C. Limberg, *Chem. Commun.* **2021**, *57*, 875–878.
[26] a) M. M. Khusniyarov, E. Bill, T. Weyhermüller, E. Bothe, K. Wieghardt, *Angew. Chem. Int. Ed.* **2011**, *50*, 1652–1655; b) M. P. Marshak, M. B. Chambers, D. G. Nocera, *Inorg. Chem.* **2012**, *51*, 11190–11197; c) J. Takaichi, Y. Morimoto, K. Ohkubo, C. Shimokawa, T. Hojo, S. Mori, H. Asahara, H. Sugimoto, N. Fujieda, N. Nishiwaki, S. Fukuzumi, S. Itoh, *Inorg. Chem.* **2014**, *53*, 6159–6169; d) C. Camp, J. Arnold, *Dalton Trans.* **2016**, *45*, 14462–14498.
[27] A. R. Sadique, W. W. Brennessel, P. L. Holland, *Inorg. Chem.* **2008**, *47*, 784–786.
[28] C. E. Kefalidis, A. Stasch, C. Jones, L. Maron, *Chem. Commun.* **2014**, *50*, 12318–12321.
[29] N. A. Eckert, A. Dinescu, T. R. Cundari, P. L. Holland, *Inorg. Chem.* **2005**, *44*, 7702–7704.
[30] G. A. Bain, J. F. Berry, *J. Chem. Educ.* **2008**, *85*, 532.
[31] a) F. Neese, *Wiley Interdiscip. Rev.: Comput. Mol. Sci.* **2012**, *2*, 73–78; b) F. Neese, *Wiley Interdiscip. Rev.: Comput. Mol. Sci.* **2017**, e1327.
[32] a) A. D. Becke, *Phys. Rev. A* **1988**, *38*, 3098; b) C. Lee, W. Yang, R. G. Parr, *Phys. Rev. B* **1988**, *37*, 785; c) A. D. Becke, *J. Chem. Phys.* **1993**, *98*, 5648.
[33] a) S. Grimme, S. Ehrlich, L. Goerigk, *J. Comput. Chem.* **2011**, *32*, 1456–1465; b) S. Grimme, J. Antony, S. Ehrlich, H. Krieg, *J. Chem. Phys.* **2010**, *132*, 154104.
[34] F. Weigend, R. Ahlrichs, *Phys. Chem. Chem. Phys.* **2005**, *7*, 3297.
[35] F. Weigend, *Phys. Chem. Chem. Phys.* **2006**, *8*, 1057.
[36] F. Weigend, R. Ahlrichs, *Phys. Chem. Chem. Phys.* **2005**, *7*, 3297.
[37] G. M. Sheldrick, SADABS **1996**, University of Göttingen, Germany.
[38] G. M. Sheldrick, *Acta Crystallogr. Sect. A* **2015**, *71*, 3.
[39] G. M. Sheldrick, *Acta Crystallogr. Sect. C* **2015**, *71*, 3.
[40] C. B. Hübschle, G. M. Sheldrick, B. Dittrich, *J. Appl. Crystallogr.* **2011**, *44*, 1281–1284.
[41] A. L. Spek, *Acta Crystallogr. D, Biological crystallography* **2009**, *65*, 148.

Manuscript received: October 11, 2024
Accepted manuscript online: December 5, 2024
Version of record online: December 17, 2024